Proceedings of CONF-MCEE 2027 Symposium: Advanced Nanomaterials and 2D Materials: Synthesis, Modeling, and Applications
DOI: 10.54254/2755-2721/2027.AD38705

Perovskite Oxides: Synthesis Strategies and Advances in Photoelectrocatalytic Applications

Canyi Tu

School of Materials Science and Engineering, Shanghai University, Shanghai, China
sophiatu@shu.edu.cn

Abstract. The depletion of fossil fuels and the resulting environmental burden have increased interest in photocatalytic routes for converting solar energy into storable chemical energy. Their overall performance depends strongly on the intrinsic physicochemical properties of the photoanode material. Conventional wide-bandgap semiconductors are limited by restricted visible-light absorption and rapid charge-carrier recombination that lowers quantum efficiency and hinders practical implementation. Perovskite oxides offer adjustable crystal structures, flexible metal valence states and useful redox properties, making them promising candidates for addressing these critical limitations. This review examines the crystal structures and photocatalytic mechanisms of perovskite oxides and compares how sol–gel, solid-state, coprecipitation, and hydrothermal synthesis affect grain size, microstructure, and surface defects. It also discusses their emerging applications in electrocatalytic nitrate reduction to ammonia and photocatalytic selective oxidation of organic substrates. The review relates synthesis conditions to carrier separation and surface reaction barriers, providing a solid basis for designing stable, efficient photocatalytic systems toward scalable solar-to-chemical conversion.

Keywords: Perovskite Oxide, Synthesis Methods, Photoelectrocatalysis

1. Introduction

The widespread use of fossil fuels has intensified the energy crisis and increased CO_2 emissions, with serious consequences for climate and the environment. Solar-driven photocatalysis, including water splitting for hydrogen production, CO_2 reduction to fuels, and the degradation of organic pollutants, is one route to cleaner energy conversion and environmental remediation [1]. A useful photocatalyst must absorb a broad portion of the spectrum, separate and transport photo-generated carriers efficiently, and provide enough active surface sites. Traditional materials such as TiO_2 and ZnO do not fully meet these requirements because they respond to a limited wavelength range, recombine charges readily, show slow surface kinetics, and may undergo photocorrosion under illumination. Their solar conversion efficiencies therefore remain below the level needed for industrial use [2]. Developing materials that combine wider absorption, effective carrier separation, and physicochemical stability remains a central challenge. Perovskites are also being examined for electrocatalytic nitrate treatment, where nitrate pollution can be reduced while nitrogen-containing products are recovered [3].

© 2026 The Authors. This is an open access article distributed under the terms of the Creative Commons Attribution License 4.0 (https://creativecommons.org/licenses/by/4.0/).

DOI: 10.54254/2755-2721/2027.AD38705

Perovskite composite oxides are compounds related structurally to the mineral $CaTiO_3$ and are commonly described by the formula ABO_3 (Figure 1). The smaller B-site cation, often a transition metal, is surrounded by six oxygen ions in a BO_6 octahedron. A larger rare-earth or alkaline-earth cation occupies the cavity between these octahedra and is coordinated by twelve oxygen ions [4, 5]. This framework is resistant to sintering and can remain stable in redox environments and in the presence of reaction products. Oxygen migration through the lattice contributes to oxidation activity, while the surface atomic arrangement and surface energy affect active sites and the adsorption and desorption of reactants. Controlling the structure and surface therefore offers a way to improve catalytic performance [6, 7].

The physicochemical properties of perovskite catalysts depend strongly on how they are prepared. Changes in the synthesis route can alter morphology, crystal structure, and surface groups. Common routes include sol–gel synthesis, coprecipitation, microemulsion synthesis, hydrothermal or solvothermal treatment, templating, and the Pechini method [8]. Because perovskite composite oxides combine redox activity, thermal stability, oxygen-transfer capability, and compositional flexibility, they have been studied in thermocatalysis, photocatalysis, electrocatalysis, photocatalytic electrolysis, and photothermal catalysis [2, 7].

This review compares the main synthesis routes for perovskite oxides and considers how each route affects grain size, microstructure, lattice distortion, oxygen-vacancy concentration, specific surface area, and interfacial defects. These features are closely related to carrier recombination, surface reaction barriers, and resistance to photodegradation. The review therefore connects preparation conditions with recent photocatalytic applications and the performance limitations that those applications must address.

2. Crystal structures and photocatalytic properties of perovskite oxides

2.1. Structural features of perovskite oxides

The name perovskite oxide refers to the similarity between the ABO_3 framework and the crystal structure of $CaTiO_3$. These materials are widely studied for photocatalysis because their band structures can be adjusted and their surfaces can support charge separation and catalytic reactions [5]. An ideal perovskite has a cubic unit cell with space group Pm3m. The B-site cation lies at the centre of a BO_6 octahedron and is coordinated by six oxygen anions, while the A-site cation occupies the larger interstitial position between the octahedra (Figure 1). Alkali metals, alkaline-earth metals, and lanthanides can occupy the A site, whereas transition metals commonly occupy the B site. The two sites can accommodate many elements (Figure 2), producing a broad family of perovskite oxides.

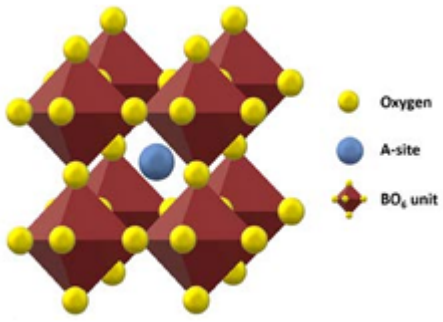


Figure 1. Schematic illustration of the ideal cubic perovskite structure model [9]

DOI: 10.54254/2755-2721/2027.AD38705

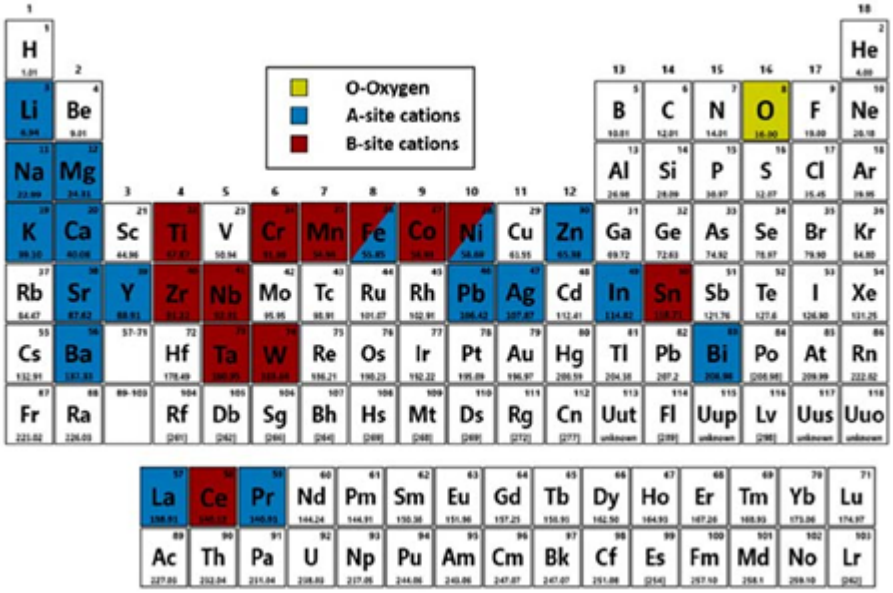


Figure 2. Elemental compositions used for the fabrication of perovskite oxides [9]

2.2. Photocatalytic properties of perovskite oxides

When illuminated with photons whose energy exceeds the bandgap, a perovskite oxide promotes electrons from the valence band (VB) to the conduction band (CB), leaving electron–hole pairs. The carriers migrate toward the surface and participate in redox reactions. Electrons can reduce oxygen to reactive oxygen species, including superoxide anions (O_2^-), hydroxyl radicals (·OH), and hydrogen peroxide (H_2O_2). Holes oxidise organic pollutants adsorbed on the surface through dehydrogenation, oxidation, and mineralisation. The pollutants are ultimately converted into less harmful products such as CO_2 and H_2O [10]. Representative band structures are shown in Figure 3.

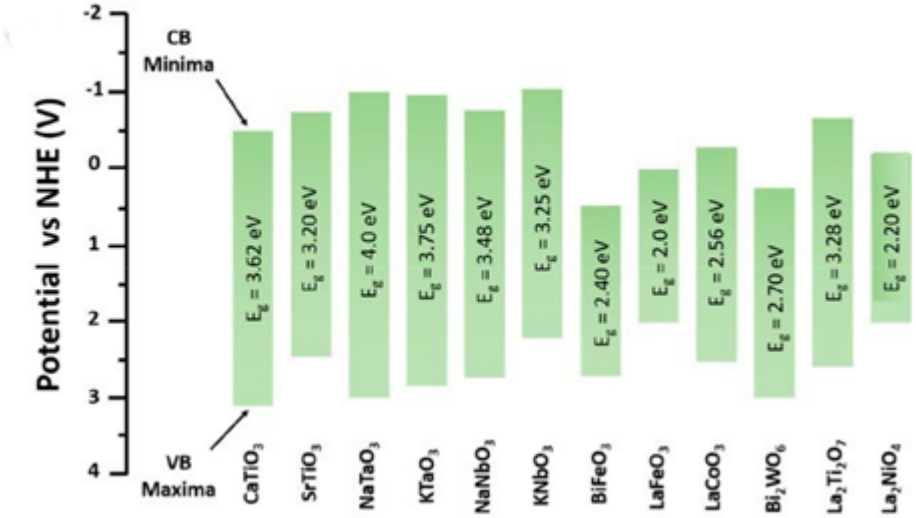


Figure 3. Energy band structure of representative perovskite oxides [9]

DOI: 10.54254/2755-2721/2027.AD38705

2.2.1. Photocatalytic reaction pathways

Photocatalysis couples light absorption with charge separation and interfacial reactions. Under ultraviolet or visible light, the catalyst produces electron–hole pairs. Carriers reaching the surface can react with adsorbed species at active sites, which initiates the desired conversion. Because their band structures and optical responses can be tuned, perovskite oxides have been investigated for water splitting, CO_2 reduction, and the degradation of antibiotics, dyes, and other persistent pollutants. CO_2 reduction is of particular interest because it offers a route for using a major greenhouse gas as a chemical feedstock and may contribute to carbon-cycle management [10].

2.2.2. Electrocatalytic properties of perovskite oxides

Electrocatalytic reactions use electrical energy to drive charge transfer at the electrode–electrolyte interface. The transferred electrons and holes promote redox reactions between species in the electrolyte and active sites on the catalyst, producing the desired products [11]. Perovskite composite oxides combine compositional flexibility, electrical conductivity, and abundant active centres. They have therefore been investigated for CO_2 reduction, coupled methane oxidation, and water electrolysis for hydrogen and oxygen production.

Electrocatalytic CO_2 reduction can recover carbon dioxide under relatively mild conditions and convert it into useful products. Its controllable operation and compatibility with clean electricity make it relevant to the goals of reaching carbon emission peaks and carbon neutrality [12].

3. Methods for the synthesis and preparation of perovskite oxides

3.1. Sol–gel method

Sol–gel synthesis is a relatively inexpensive route for producing nanomaterials with uniform composition and morphology. Metal ions coordinate with chelating agents such as ethylene glycol, EDTA, or tartaric acid to form a gel network; the reported optimum metal-ion-to-chelating-agent ratio is 1:1. The main steps are illustrated in Figure 4 [13]. The Pechini variant is frequently used because it can operate under mild conditions and offers high purity, reproducible composition, and control over the final structure. Calcination temperature, reaction time, pH, and precursor selection affect the microstructure, pore size, and specific surface area [10]. Li et al. prepared $LaMnO_3$ with citric acid and EDTA. The nanoparticles obtained from the EDTA–citric acid complex were smaller than those produced with citric acid alone, and the resulting oxide showed catalytic activity in CO_2 reduction and H_2 evolution [14].

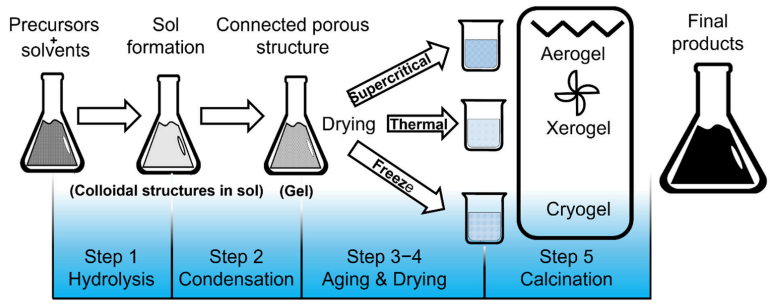


Figure 4. Schematic representation of step-by-step Sol-Gel method [13]

DOI: 10.54254/2755-2721/2027.AD38705

The stability and selectivity of ABO_3 oxides can be adjusted through the choice of A- and B-site elements or through chemical doping. Examples include $NiTiO_3$, $CoTiO_3$, $BaZrO_3$, $LaMnO_3$, $MnTiO_3$, and $PbTiO_3$ [10]. Sol–gel synthesis can also be combined with other techniques to prepare doped or nanocomposite perovskites with controlled morphology, particle size, and crystal structure.

3.2. Solid-state synthesis method

In a solid-state route, nitrates, carbonates, oxides, or related precursors are mixed in stoichiometric proportions and heated at high temperature. For perovskites, oxides or carbonates containing the A- and B-site metals are commonly ground together before calcination. Zhang et al. prepared $LaAlO_3$ by grinding equimolar aluminium oxide and lanthanum oxide at room temperature, followed by heat treatment. X-ray diffraction confirmed the rhombohedral $LaAlO_3$ phase, although weak $LaAl_{11}O_{18}$ peaks remained after sintering [15]. Abdi et al. used a solid-state route to prepare La- and Fe-doped $SrTiO_3$ and examined how dopant concentration changed its physicochemical properties. Doping lowered the bandgap from 3.2 eV to 2.72 eV and shifted the absorption edge toward shorter wavelengths. The doped samples showed higher visible-light activity, with the best result obtained for $SrTiO_3$ containing 4% Fe–La. Its activity for MO degradation was 19 times that of undoped $SrTiO_3$. The method nevertheless provides limited control over particle size, shape, and dopant distribution, which restricts its use when precise structural control is required [16].

3.3. Coprecipitation method

Coprecipitation is widely used for nanoparticle preparation. A precursor solution is added to a solvent under controlled conditions, often with a stabiliser, and supersaturation is followed by nucleation and growth. The process is shown schematically in Figure 5 [17]. Particle size and shape depend on the reaction parameters. The method is simple and inexpensive and can produce particles smaller than 100 nm. Huang et al. used N,N-dimethylacetamide (DMAC) as the solvent and tetramethylammonium hydroxide (TMAOH) as the precipitant to prepare $La_{0.6}Sr_{0.4}MnO_3$ nanoparticles. The particles were approximately 20 nm in size and had a specific surface area of 48 m^2/g [18]. Nguyen et al. prepared $YFe_{1-}_xMn_xO_3$ ($0.1 \leq x \leq 0.4$) nanopowders by hydrating Y(III), Fe(III), and Mn(II) cations in boiling water and annealing the precipitate at 800 °C for 1 hour. The product was a single-phase perovskite with a crystal size of about 23 nm, and TEM showed a uniform distribution near 20 nm [19].

DOI: 10.54254/2755-2721/2027.AD38705

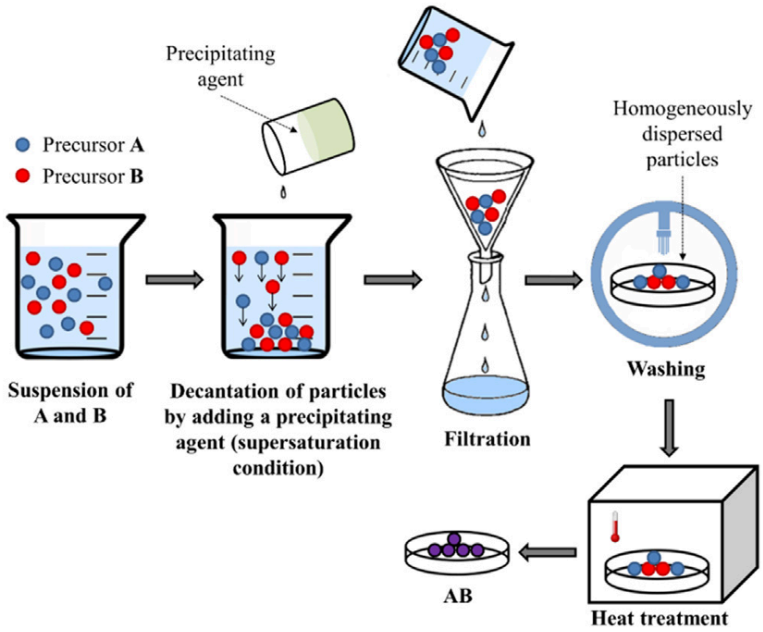


Figure 5. General schematic of the co-precipitation method [18]

3.4. Hydrothermal/solvothermal synthesis

Hydrothermal and solvothermal synthesis use water or an organic solvent, respectively, as the reaction medium in a pressurised, high-temperature process. The route can produce perovskites with high crystallinity, high purity, and relatively uniform particles. Pressure, temperature, solvent, and pH affect crystallisation and can reduce the impurity phases and defects associated with volatilisation in solid-state reactions [10]. Wang et al. prepared cubic Sr-doped $LaCrO_3$ in a one-step hydrothermal reaction at 260 °C. The particles measured 1–2 μm, and both KOH concentration and reaction temperature influenced their size and morphology [20]. Combining hydrothermal treatment with microwave heating or coprecipitation can further change the product. Biasotto et al. prepared $BiFeO_3$ by microwave-assisted hydrothermal synthesis at 180 °C for 5 minutes to 1 hour. Compared with the solid-state route, the method gave more uniform and crystalline products at the lower temperature. Short treatments produced peak splitting and minor XRD peaks associated with $Bi_2Fe_4O_9$, while a 1-hour treatment yielded a highly pure orthorhombic phase [21].

4. Applications of perovskite oxides in photocatalysis

4.1. Electrocatalytic nitrate reduction to ammonia using perovskite oxides

Electrocatalytic nitrate reduction (NO_3RR) converts nitrate in water through coupled electron–proton steps into products such as N_2, NH_3, or NO_2^-. The process is being studied in the context of renewable energy and carbon-reduction goals. Unlike biological denitrification and chemical reduction, it can operate without additional chemical reagents, offers electrical control, and can be powered by renewable electricity. Selective conversion to NH_3 also creates a route for recovering nitrogen from wastewater and producing nitrogen-containing chemicals or fertilisers. This links pollution treatment with resource recovery and avoids some of the energy and carbon costs associated with conventional Haber–Bosch ammonia production [22, 23]. The adjustable

DOI: 10.54254/2755-2721/2027.AD38705

composition and electronic structure of perovskite oxides make them candidates for NO_3RR at ambient temperature and pressure. Because the reaction involves multiple electron and proton transfers, it can also be coupled with electrochemical storage, wastewater recovery, and carbon–nitrogen coupling for urea synthesis.

4.2. Perovskite oxides for photocatalytic oxidation reactions

Photocatalytic oxidation is driven mainly by photo-generated holes. Many perovskite oxides have wide bandgaps and valence-band maxima at positive potentials near 3 eV, which can provide the oxidation potential required for several reactions. Reported applications include alkane oxidation, oxygen evolution from water splitting, degradation of organic pollutants, and selective oxidation of alcohols and aldehydes [24]. The pathways can be grouped into three types. In direct hole oxidation, holes reach the surface and transfer charge to an adsorbed substrate. In reactive-oxygen-species oxidation, holes or electrons react with adsorbed water, peroxide, or oxygen to form species such as ·OH and $\cdot O_2^-$, which then oxidise the substrate. In lattice-oxygen oxidation, photo-generated holes oxidise lattice oxygen, the resulting lattice oxygen reacts with the substrate, and the oxygen vacancy is later replenished by O_2 or another oxidant.

5. Conclusion

This review has covered the crystal structures, photocatalytic properties, synthesis routes, and photocatalytic applications of perovskite oxides. Their adjustable composition, redox chemistry, and surface active sites allow them to address some limitations of conventional catalysts. Synthesis conditions affect grain size, specific surface area, oxygen vacancies, and crystal quality, and these changes are reflected in photocatalytic performance. Current applications include nitrate-nitrogen recovery and the degradation of organic pollutants. Further work should improve synthesis control and interface engineering so that perovskite photocatalysts can be used more reliably at larger scale.

References

[1] Shindell, D., & Smith, C. J. (2019). Climate and air-quality benefits of a realistic phase-out of fossil fuels. *Nature, 573*(7774), 408–411. https://doi.org/10.1038/s41586-019-1554-z.

[2] Kou, J., Lu, C., Wang, J., Chen, Y., Xu, Z., & Varma, R. S. (2017). Selectivity enhancement in heterogeneous photocatalytic transformations. *Chemical Reviews, 117*(3), 1445–1514. https://doi.org/10.1021/acs.chemrev.6b00396.

[3] Xu, M., Dong, S., Guo, H., Tao, Z., Jeon, Y., & et al. (2025). Defective perovskite supported palladium-nickel nanocatalyst for effective electrochemical nitrate reduction. *Applied Catalysis B: Environment and Energy, 375*, 125433. https://doi.org/10.1016/j.apcatb.2025.125433.

[4] Grabowska, E. (2016). Selected perovskite oxides: Characterization, preparation and photocatalytic properties—A review. *Applied Catalysis B: Environmental, 186*, 97–126. https://doi.org/10.1016/j.apcatb.2015.12.035.

[5] Peña, M. A., & Fierro, J. L. G. (2001). Chemical structures and performance of perovskite oxides. *Chemical Reviews, 101*(7), 1981–2017. https://doi.org/10.1021/cr980129f.

[6] Kobayashi, M., Katsuraya, R., Nara, T., Tomita, Y., Nakano, H., & Kamegashira, N. (2006). Phase behavior and crystal structure of perovskite-type rare earth complex oxides. *Journal of Rare Earths, 24*(6), 668–672. https://doi.org/10.1016/S1002-0721(07)60006-4.

[7] Fu, C. J., Ma, Q., Gao, L., & Li, S. (2023). Recent advances in perovskite oxides electrocatalysts: Ordered perovskites, cations segregation and exsolution. *ChemCatChem, 15*(11), e202300389. https://doi.org/10.1002/cctc.202300389.

[8] Zhu, J., Li, H., Zhong, L., Xiao, P., Xu, X., Yang, X., Zhao, Z., & Li, J. (2014). Perovskite oxides: Preparation, characterizations, and applications in heterogeneous catalysis. *ACS Catalysis, 4*, 2917–2940. https://doi.org/10.1021/cs500606g.

DOI: 10.54254/2755-2721/2027.AD38705

[9] Kumar, A., Kumar, A., & Krishnan, V. (2020). Perovskite oxide based materials for energy and environment-oriented photocatalysis. *ACS Catalysis, 10*, 10253–10315. https://doi.org/10.1021/acscatal.0c02947.

[10] Kumar, R., Kumar, D., Lokhande, P. E., Kadam, V., Jagtap, C., Vedapathak, A. S., Singh, K., Mishra, Y. K., & Kaushik, A. (2025). Emergence of perovskites oxides as advanced photocatalysts for energy and environmental remediation application. *Coordination Chemistry Reviews, 11*, 216556. https://doi.org/10.1016/j.ccr.2025.216556.

[11] Wu, H., Huang, Q., Shi, Y., Chang, J., & Lu, S. (2023). Electrocatalytic water splitting: Mechanism and electrocatalyst design. *Nano Research, 16*, 9142–9157. https://doi.org/10.1007/s12274-023-5502-8.

[12] Lv, L., Lu, R., Zhu, J., Yu, R., Zhang, W., Cui, E., Chen, X., Dai, Y., Cui, L., Li, J., Zhou, L., Chen, W., Wang, Z., & Mai, L. (2023). Coordinating the edge defects of bismuth with sulfur for enhanced CO_2 electroreduction to formate. *Angewandte Chemie International Edition, 62*, e202303117. https://doi.org/10.1002/anie.202303117.

[13] Navas, D., Fuentes, S., Castro-Alvarez, A., & Chavez-Angel, E. (2021). Review on sol-gel synthesis of perovskite and oxide nanomaterials. *Gels, 7*, 275. https://doi.org/10.3390/gels7040275.

[14] Li, C., Yu, Z., Liu, H., & Chen, K. (2018). High surface area $LaMnO_3$ nanoparticles enhancing electrochemical catalytic activity for rechargeable lithium-air batteries. *Journal of Physics and Chemistry of Solids, 113*, 151-156. https://doi.org/10.1016/j.jpcs.2017.10.039.

[15] Zhang, Q., & Saito, F. (2004). Mechanochemical synthesis of lanthanum aluminate by grinding lanthanum oxide with transition alumina. *Journal of the American Ceramic Society, 83*, 439-441. https://doi.org/10.1111/j.1151-2916.2000.tb01215.x.

[16] Abdi, M., Mahdikhah, V., & Sheibani, S. (2020). Visible light photocatalytic performance of La-Fe co-doped $SrTiO_3$ perovskite powder. *Optical Materials, 102*, 109803. https://doi.org/10.1016/j.optmat.2020.109803.

[17] Athayde, D. D., Souza, D. F., Silva, A. M. A., Vasconcelos, D., Nunes, E. H. M., Diniz da Costa, J. C., & Vasconcelos, W. L. (2016). Review of perovskite ceramic synthesis and membrane preparation methods. *Ceramics International, 42*, 6555-6571. https://doi.org/10.1016/j.ceramint.2016.01.130.

[18] Huang, F., Sun, X., Zheng, Y., Xiao, Y., & Zheng, Y. (2018). Facile coprecipitation synthesis of $La_{0.6}Sr_{0.4}MnO_3$ perovskites with high surface area. *Materials Letters, 210*, 287-290. https://doi.org/10.1016/j.matlet.2017.09.048.

[19] Nguyen, A. T., Pham, V. N. T., Nguyen, T. T. L., Mittova, V. O., Vo, Q. M., Berezhnaya, M. V., Mittova, I. Y., Do, T. H., & Chau, H. D. (2019). Crystal structure and magnetic properties of perovskite $YFe_{1-x}Mn_xO_3$ nanopowders synthesized by coprecipitation method. *Solid State Sciences, 96*, 105922. https://doi.org/10.1016/j.solidstatesciences.2019.06.011.

[20] Wang, S., Huang, K., Zheng, B., Zhang, J., & Feng, S. (2013). Mild hydrothermal synthesis and physical property of perovskite Sr doped $LaCrO_3$. *Materials Letters, 101*, 86-89. https://doi.org/10.1016/j.matlet.2013.03.083.

[21] Biasotto, G., Simoes, A. Z., Foschini, C. R., Zaghete, M. A., Varela, J. A., & Longo, E. (2011). Microwave-hydrothermal synthesis of perovskite bismuth ferrite nanoparticles. *Materials Research Bulletin, 46*, 2543-2547. https://doi.org/10.1016/j.materresbull.2011.08.010.

[22] Wu, X., Wang, X., Wu, Y., Xu, H., Li, Z., Hong, R., Rigby, K., Wu, Z., & Kim, J.-H. (2025). Bilayer electrified-membrane with pair-atom tin catalysts for near-complete conversion of low concentration nitrate to dinitrogen. *Nature Communications, 16*, 1122. https://doi.org/10.1038/s41467-025-56102-7.

[23] Wu, Z., Kang, X., Wang, S., Song, Y., Xie, F., Duan, X., & Yang, J. (2024). Co-catalytic metal-support interactions design on single-atom alloy for boosted electro reduction of nitrate to nitrogen. *Advanced Functional Materials, 34*(45), 2406917. https://doi.org/10.1002/adfm.202406917.

[24] Wang, K., Han, C., Shao, Z., Qiu, J., Wang, S., & Liu, S. (2021). Perovskite oxide catalysts for advanced oxidation reactions. *Advanced Functional Materials, 31*(30), 2102089. https://doi.org/10.1002/adfm.202102089.